2022 International Symposium on Nonlinear Theory and Its Applications,
NOLTA2022, Virtual, December 12-15, 2022

A generalized ergodic cellular automaton model of central pattern generator and its bifurcation analyses induced by chopper type mixed gaits

Jumpei Kamitoko† and Hiroyuki Torikai‡

†Graduate School of Science and Engineering, Hosei University
3-7-2 Kajino-cho, Koganei, Tokyo 184-8584, Japan
Email: jumpei.kamitoko.6a@stu.hosei.ac.jp, torikai@hosei.ac.jp

Abstract—In this paper, we propose a generalized ergodic cellular automaton model of a central pattern generator. The proposed model can realize synchronization phenomena, which can realize typical gaits of a quadruped robot. It is shown that by mixing coupling matrices based on a chopper manner, the proposed model can realize mixed gaits of the quadruped robot depending on the ratios of the matrices in the chopper. Also, it is shown that the proposed model is more hardware-efficient compared to a straightforward implementation of an ordinary differential equation central pattern generator model.

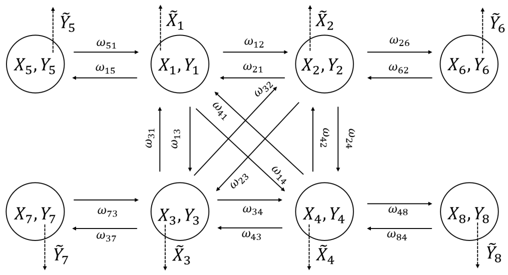

Figure 1: Schematic diagram of ergodic cellular automaton CPG model [3].

1. Introduction

Multilegged creatures such as ants and spiders, and legless creatures such as snakes and fish can perform various types of walking, crawling, and swimming locomotion using flexor and extensor muscles that are moved in rhythmic patterns. These rhythmic patterns are thought to be generated by the central pattern generator (CPG) in the central nervous system [1][2]. In the previous study [3], an ergodic cellular automaton CPG model to realize some typical gaits of a quadruped robot was designed. On the other hand, in this study, the circuit structure of the ergodic cellular automaton CPG model is generalized so that its coupling matrix can be changed in a chopper manner. It is shown that the proposed CPG model can realize various gaits of the quadruped robot by adjusting the chopper ratio of the coupling matrices.

2. Ergodic Cellular Automaton CPG

In this section, the ergodic cellular automaton CPG model [3] is introduced. Fig. 1 shows a schematic diagram of the CPG model. The CPG model consists of eight ergodic cellular automaton oscillators. Each i-th oscillator has six registers, which store discrete state variables X_i and Y_i and discrete auxiliary variables P_i, Q_i, V_i, and U_i. These variables are defined as follows.

$$X_i \in Z_N = \{0, \dots, N-1\}, Y_i \in Z_N,$$
$$P_i \in Z_M = \{0, \dots, M-1\}, Q_i, V_i, U_i \in Z_M, \tag{1}$$

ORCID iDs First Author: 0000-0002-4786-5509, Second Author: 0000-0003-2795-9628.

where X_i and Y_i work as state variables, and P_i, Q_i, V_i, and U_i work as state-dependent frequency dividers. The oscillator receives a periodic clock $C_i(t) = \sum_{n=0}^{\infty} p(t-nT_{Ci})$, where $p(t) = 1$ if $t = 0$ and $p(t) = 0$ if $t \neq 0$. In addition, the oscillator receives binary switch signals $S_{Xi}(t) = \sum_{n=0}^{\infty} q(t-nT_{Xi} - \Phi_{Xi}, W_{Xi})$ and $S_{Yi}(t) = \sum_{n=0}^{\infty} q(t - nT_{Yi} - \Phi_{Yi}, W_{Yi})$, where $q(t) = 1$ if $t \in [0, W]$, $q(t) = 0$ if $t \notin [0, W]$, T_{Xi} and T_{Yi} are periods, and W_{Xi} and W_{Yi} are pulse durations. When the clock $C_i(t) = 1$ arrives, the state variables X_i and Y_i undergo the following transitions.

$$\begin{aligned} X_i(t^+) &= X_i(t) + S_{Xi}(t)\mathcal{F}_X(X_i(t), Y_i(t), P_i(t)) \\ &\quad + S_{Gi}(t)\mathcal{G}_i(\boldsymbol{X}(t), \boldsymbol{V}(t)), \\ Y_i(t^+) &= Y_i(t) + S_{Yi}(t)\mathcal{F}_Y(X_i(t), Y_i(t), Q_i(t)) \\ &\quad + S_{Gi}(t)\mathcal{G}_i(\boldsymbol{Y}(t), \boldsymbol{U}(t)), \end{aligned} \tag{2}$$

where $\mathcal{F}_X \in \{-1, 0, 1\}$ and $\mathcal{F}_Y \in \{-1, 0, 1\}$ are discrete functions designed to realize appropriate oscillation. The clock $C_i(t)$ induces transitions of the discrete auxiliary variables P_i, Q_i, V_i, and U_i so that these variables work as state-dependent frequency dividers. In addition, $\mathcal{G}_i \in \{-1, 0, 1\}$ is a discrete function, which couples the oscillators, where $\boldsymbol{X} = (X_1, ...X_8)$, $\boldsymbol{Y} = (Y_1, ...Y_8)$, $\boldsymbol{V} = (V_1, ...V_8)$, and $\boldsymbol{U} = (U_1, ..., U_8)$.

3. Chopper Type Mixed Gaits

In this section, the CPG model is generalized so that the discrete function $\mathcal{G}_i$ for the coupling is chopper type time-

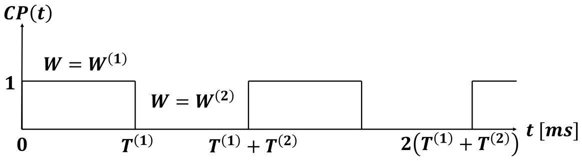

Figure 2: Chopper signal $CP(t)$ that changes of the coupling matrix $\boldsymbol{W}$.

variant as follows.

$$\mathcal{G}_i(\boldsymbol{X}(t), \boldsymbol{V}(t), \boldsymbol{W}^{(1)}, \boldsymbol{W}^{(2)}, CP(t)) = \begin{cases} (\sigma \sum_{j=1}^{8} w_{ij}^{(1)}(X_j - N/2))^{-1} & \text{if } CP_i(t) = 1, \\ (\sigma \sum_{j=1}^{8} w_{ij}^{(2)}(X_j - N/2))^{-1} & \text{if } CP_i(t) = 0, \end{cases} \quad (3)$$

where

$$\boldsymbol{W}^{(k)} = \begin{pmatrix} w_{1,1}^{(k)} & w_{1,2}^{(k)} & \cdots & w_{1,8}^{(k)} \\ w_{2,1}^{(k)} & w_{2,2}^{(k)} & \cdots & w_{2,8}^{(k)} \\ \vdots & \vdots & \ddots & \vdots \\ w_{8,1}^{(k)} & w_{8,2}^{(k)} & \cdots & w_{8,8}^{(k)} \end{pmatrix}, \quad (4)$$

$$CP(t) = \begin{cases} 1 & \text{if } t \pmod{T^{(1)} + T^{(2)}} \leq T^{(1)}, \\ 0 & \text{if } t \pmod{T^{(1)} + T^{(2)}} > T^{(1)}. \end{cases} \quad (5)$$

The signal $CP(t)$ is used to realize chopper type mixing of the two coupling matrices $\boldsymbol{W}^{(1)}$ and $\boldsymbol{W}^{(2)}$ (see Fig. 2), where the period $T^{(1)}+T^{(2)}$ of the chopper signal $CP(t)$ is assumed to be much shorter than oscillation periods of the ergodic cellular automaton oscillators. In this paper, the following two coupling matrices are used.

$$\boldsymbol{W}^{(1)} = \boldsymbol{W}^{F} = \begin{pmatrix} 0 & -1 & -1 & 1 & 2 & 0 & 0 & 0 \\ -1 & 0 & 1 & -1 & 0 & 2 & 0 & 0 \\ -1 & 1 & 0 & -1 & 0 & 0 & 2 & 0 \\ 1 & -1 & -1 & 0 & 0 & 0 & 0 & 2 \\ 2 & 0 & 0 & 0 & 0 & 0 & 0 & 0 \\ 0 & 2 & 0 & 0 & 0 & 0 & 0 & 0 \\ 0 & 0 & 2 & 0 & 0 & 0 & 0 & 0 \\ 0 & 0 & 0 & 2 & 0 & 0 & 0 & 0 \end{pmatrix} \quad (6)$$

$$\boldsymbol{W}^{(2)} = \boldsymbol{W}^{R} = \begin{pmatrix} 0 & 1 & -1 & -1 & 2 & 0 & 0 & 0 \\ 1 & 0 & -1 & -1 & 0 & -2 & 0 & 0 \\ -1 & -1 & 0 & 1 & 0 & 0 & 2 & 0 \\ -1 & -1 & 1 & 0 & 0 & 0 & 0 & -2 \\ 2 & 0 & 0 & 0 & 0 & 0 & 0 & 0 \\ 0 & -2 & 0 & 0 & 0 & 0 & 0 & 0 \\ 0 & 0 & 2 & 0 & 0 & 0 & 0 & 0 \\ 0 & 0 & 0 & -2 & 0 & 0 & 0 & 0 \end{pmatrix} \quad (7)$$

It will be confirmed in the next section that the coupling matrices $\boldsymbol{W}^{R}$ and $\boldsymbol{W}^{F}$ realize the forward walk and rightward rotation of a quadruped robot. Note that the main purpose of this study is to analyze the effects of choppering of these matrices. To analyze the effects of the choppering, the following chopper rate T_R is introduced.

$$T_R = \frac{T^{(2)}}{T^{(1)} + T^{(2)}}. \quad (8)$$

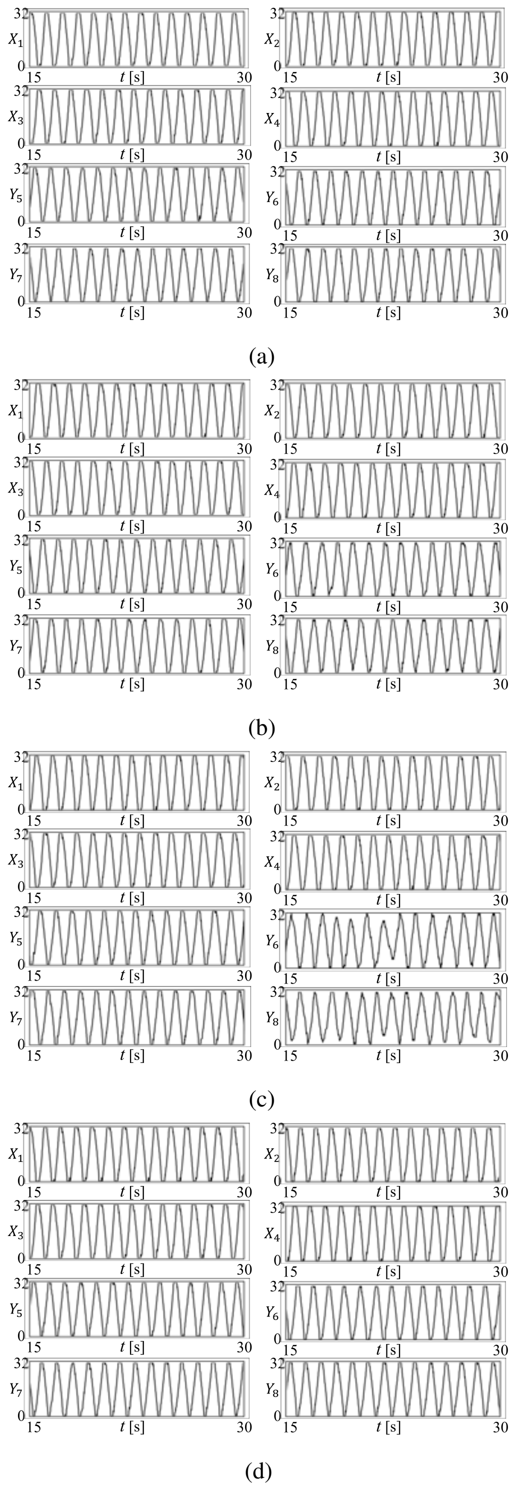

Figure 3: Time waveforms of the ergodic cellular automaton CPG model. (a) $T_R = 0.0$. (b) $T_R = 0.2$. (c) $T_R = 0.5$. (d) $T_R = 1.0$.

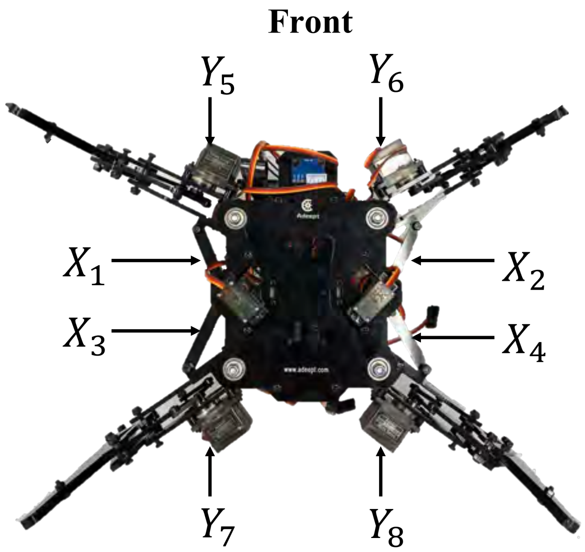

Figure 4: Quadruped robot controlled by the ergodic cellular automaton CPG implemented in the FPGA.

Fig. 3 shows typical time waveforms of the ergodic cellular automaton CPG model for some values of the chopper rate T_R as follows.

- In the case of Fig. 3(a), the chopper rate T_R is 0.0. This corresponds to $\boldsymbol{W} = \boldsymbol{W}^F$.
- In the case of Figs. 3(b) and (c), the chopper rates T_R are 0.2 and 0.5, respectively. In these cases, the coupling matrix $\boldsymbol{W}$ is given by mixing $\boldsymbol{W}^F$ and $\boldsymbol{W}^R$ in the chopper manner.
- In the case of Fig. 3(d), the chopper rate T_R is 1.0. This corresponds to $\boldsymbol{W} = \boldsymbol{W}^R$.

In the next section, it is shown that the gait of a quadruped robot undergoes bifurcations by changing the chopper rate T_R.

4. FPGA Implementation of CPG and Bifurcations of Robot Gaits

The dynamics of the ergodic cellular automaton CPG were written in a register transfer level Verilog-HDL code, which was compiled by Xilinx's design suite Vivado 2020.1. The generated bitstream file was used to implement Xilinx's field programmable gate array (FPGA) device XC7A35T-1CPG236C. As shown in Fig. 4, the FPGA was mounted on Adeept's quadruped robot Dark Paw. Fig. 5(a), (b), (c), and (d) shows gaits of the robot corresponding to the time waveforms in Fig. 3(a), (b), (c), and (d), respectively as follows.

- In the case of Fig. 5(a), the chopper rate T_R is 0.0. In this case, the robot realizes a forward walk.

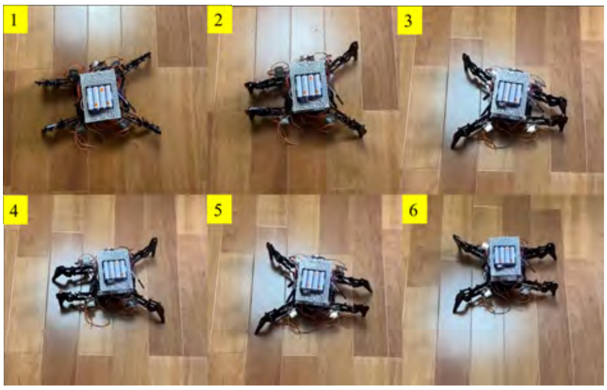

(a)

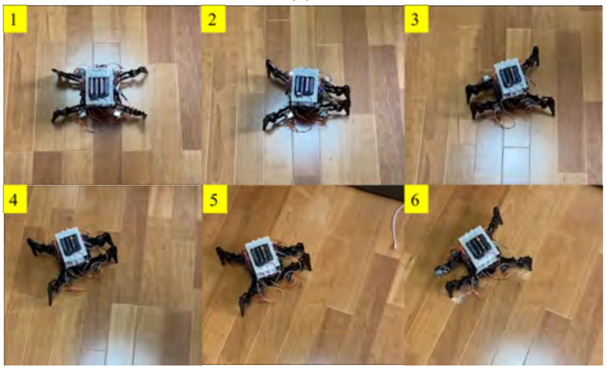

(b)

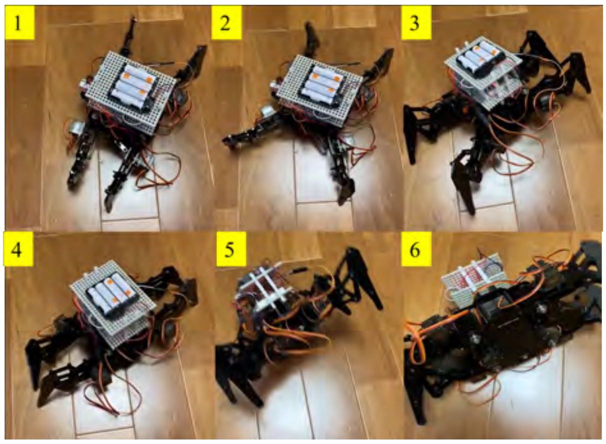

(c)

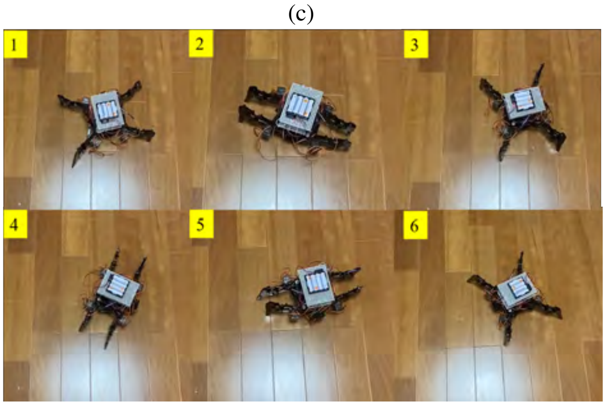

(d)

Figure 5: Gaits of the quadruped robot. (a) T_R = 0.0. (b) T_R = 0.2. (c) T_R = 0.5. (d) T_R = 1.0.

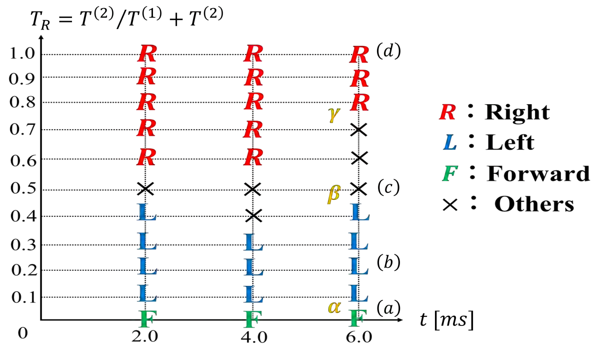

Figure 6: Bifurcation diagram of the gaits of the quadruped robot. (a)-(d) correspond to Figs. 3(a)-(d), respectivily.

- In the case of Fig. 5(b), the chopper rate T_R is 0.2. In this case, the robot realizes a leftward walk. Note that the coupling matrix $\boldsymbol{W}$ is given by mixing the matrices $\boldsymbol{W}^F$ and $\boldsymbol{W}^R$ for the forward walk and the rightward rotation, i.e., the coupling matrix $\boldsymbol{W}$ includes no factor for leftward walk but realizes the leftward walk.
- In the case of Fig. 5(c), the chopper rate T_R is 0.5. In this case, the robot realizes a complicated gait including falling down.
- In the case of Fig. 5(d), the chopper rate T_R is 1.0. In this case, the robot realizes a rightward rotation.

Fig. 6 shows a bifurcation diagram of the gaits of the quadruped robot. It can be seen that the robot undergoes the following bifurcations.

- The forward gait is changed to leftward walk by increasing the chopper rate T_R near the point α.
- The leftward walk is changed to the complicated gait including the falling down by increasing the chopper rate T_R near the point β.
- The complicated gait including the falling down is changed to the rightward rotation by increasing the chopper rate T_R near the point γ.

Detailed analyses of the occurrence mechanisms of these bifurcations are now under intensive investigations and will be presented in the conference. Table 1 shows comparisons of the ergodic cellular automaton CPG model and a differential equation CPG model [4], where the differential equation model was implemented in the same FPGA device by using the forward Euler formula. It can be seen that the ergodic cellular automaton CPG model is more hardware efficient.

5. Conclusions

In this study, the gait of the quadruped robot was realized using the ergodic cellular automaton CPG, and it was confirmed that bifurcation phenomenon of the gaits occurred by switching the coupling matrix in the chopper manner. This study also compared the ergodic cellular automaton model with the conventional differential equation model. As a result, the number of LUTs was reduced by about 35%, the number of FFs was increased by about 60%, and power consumption was reduced by about 40%, where note that the number of transistors used to implement the FF is much smaller than that used to implement the LUT. Future work includes (a) the application of ergodic cellular automaton CPG to posture control using flexor and extensor muscles, and (b) analysis of synchronization phenomena for various time-varying coupling weights like [6]. This work was supported by SCAT and KAKENHI Grant Number 21H03515.

Table 1: Comparisons.

	Ergodic cellular automaton CPG	Hopf CPG
# LUT	12600	19529
# FF	1602	617
Power (W)	0.099	0.162

References

[1] E. Kandel, et al., Principales of Neural Science, McGraw-Hill, 4th ed, 2000.

[2] S. Grillner, Neurobiological bases on of rhythmic motor acts in vertebrates, Science, Vol. 228 No.4969, pp. 143-149, 1985.

[3] S. Komaki, K. Takeda and H. Torikai, A Novel Ergodic Discrete Difference Equation Model of Central Pattern Generator: Theoretical Analysis and Efficient Implementation, IEEE TCAS II, 2021 (Early Access).

[4] J. Yu, M. Tan, J. Chen, and J. Zhang, A Surveyon CPG-Inspired Control Models and System Implementation, IEEE Transactins on Neural Networks and Leaning Systems, Vol. 21, pp. 441-456,2014.

[5] K. Takeda and H. Torikai, A novel hardware-efficient CPG model for a hexapod robot basedon nonlinear dynamics of coupled asynchronouscellular automaton oscillators, Proc. of The 2019 International Joint Conference on NeuralNetworks, N-19758, 2019.

[6] S. Anzai, T. Suzuki, T. Saito, Dynamic binary neural networks with time-variant parameters and switching of desired periodic orbits, Neurocomputing, Volume 457, 2021.